

1 Running head: Urban soil scaling

2

3

4

5 **HIERARCHICAL BAYESIAN SCALING OF SOIL PROPERTIES ACROSS URBAN,**

6 **AGRICULTURAL, AND DESERT ECOSYSTEMS**

7

8 Kaye, J.P.^{1,8}, Majumdar, A.², Gries, C.³, Buyantuyev, A.³, Grimm, N.B.⁴, Hope, D.³,

9 Jenerette, D.⁵, Zhu, W.⁶, and L. Baker⁷.

10

11

12

13 ¹Department of Crop and Soil Sciences, Pennsylvania State Univ., University Park, PA 16802

14 ²Department of Mathematics and Statistics at Arizona State University, Tempe, AZ, 85287,

15 ³Global Institute of Sustainability, Arizona State University, Tempe, AZ 85287,

16 ⁴School of Life Sciences, Arizona State University, Tempe, AZ 85287,

17 ⁵ Department of Botany and Plant Sciences, University of California, Riverside, CA 92521,

18 ⁶ Department of Biological Science, State University of New York, Binghamton, NY 13902.

19 ⁷ Minnesota Water Resources Center, St. Paul, MN 55108.

20 ⁸Corresponding author: jpk12@psu.edu; phone: 814-863-1614; fax: 814-865-7043

21 ABSTRACT

22 Ecologists increasingly use plot-scale data to inform research and policy related to regional and
23 global environmental change. For soil chemistry research, scaling from the plot to the region is
24 especially difficult due to high spatial variability at all scales. We used a hierarchical Bayesian
25 model of plot-scale soil nutrient pools to predict storage of soil organic carbon (oC), inorganic
26 carbon (iC), total nitrogen (N), and available phosphorus (avP) in a 6400 km² area including the
27 Phoenix, AZ metropolitan area and its desert and agricultural surroundings. The Bayesian
28 approach was compared to a traditional approach that multiplied mean values for urban mesic
29 residential, urban xeric residential, non-residential urban, agricultural, and desert areas by the
30 aerial coverage of each land-use type. Both approaches suggest that oC, N, and avP are highly
31 correlated with each other and are higher (in g/m²) in mesic residential and agricultural areas
32 than in deserts or xeric residential areas. In addition to traditional biophysical variables, cultural
33 variables related to impervious surface cover, tree cover, and turfgrass cover were significant in
34 regression models predicting the regional distribution of soil properties. We estimate that 1140
35 Gg of oC have accumulated in human-dominated soils of this region, but a significant portion of
36 this new C has a very short mean residence time in mesic lawns and agricultural soils. For N, we
37 estimate that 130 Gg have accumulated in soils, which explains a significant portion of “missing
38 N” observed in the regional N budget. Predictions for iC differed between the approaches
39 because the Bayesian approach predicted iC as a function of elevation while the traditional
40 approach used only land use. We suggest that Bayesian scaling enables models that are flexible
41 enough to accommodate the diverse factors controlling soil chemistry in desert, urban, and
42 agricultural ecosystems, and thus, may represent an important tool for ecological scaling that
43 spans land-use types. Urban planners and city managers attempting to reduce C emissions and

44 N pollution should consider ways that landscape choices and impervious surface cover affect
45 city-wide soil C and N storage.

46

47 Key words: urban ecology; hierarchical Bayes; scaling; soil organic carbon; soil inorganic
48 carbon; soil nitrogen; soil phosphorus; Phoenix, Arizona; CAP LTER

49 INTRODUCTION

50 Over the past several decades, scaling has been an illuminating area for development of
51 ecological theory and application. Theoretical advances explored cross-scale linkages in which
52 patterns observed at one scale develop from processes operating at other scales (Levin 1992), and,
53 paradoxically, “scaling rules” that describe how some ecological phenomena vary predictably
54 across multiple scales (Brown et al. 2004). These theoretical advances are applied to a wide
55 variety of environmental problems. In ecosystem ecology one of the most common applications
56 has been to link short-term and small-plot measurements to problems of regional or global
57 environmental change (Davidson and LeFebvre 1993; Jenerette et al. 2006). In this paper, we
58 advance the theory and application of scaling in ecology by using a hierarchical Bayesian
59 framework to scale small-plot measurements of soil carbon, nitrogen, and phosphorus to predict
60 their distribution across a mixed land-use region of central Arizona, USA.

61 Ecosystems research is particularly amenable to scaling across land-use types because
62 pools and fluxes of energy and nutrients can be expressed in the same units (mass of C, N, P,
63 etc.) in all ecosystems. Scaling up from plots is important for a variety of reasons. For C, soils
64 are the largest terrestrial pool, and regional changes in this large pool have been linked to
65 changes in global atmospheric chemistry (Pacala et al. 2001). Carbon scaling will become
66 increasingly important in urbanized regions as municipalities initiate city-scale versions of the
67 Kyoto Protocol (Ellison 2006, Reppert 2006). For N, humans have doubled the amount of
68 reactive N in the biosphere, and soils are an important sink for this new reactive N with
69 implications for biotic communities and water and air quality (Aber et al. 1998). For P, regional
70 distributions link pedology and atmospheric dust transport to plant productivity (Okin et al.
71 2004). Ptacnik et al. (2005) hypothesize that humans may decouple C, N, and P cycling in urban

72 regions because the stoichiometry (C:N:P ratio) of human mediated atmospheric transport
73 diverges greatly from the ambient stoichiometry of element inputs to ecosystems.

74 Ecosystem scientists have used a variety of models to scale soil carbon and nutrient pools
75 from the plot to the region (Burke 2000). Many are based on the use of soil surveys that couple a
76 limited number of chemical analyses (sometimes one profile per soil series) with aerial photos
77 and networks of field soil pits and cores to produce maps of soil types at regional scales. To
78 calculate regional soil chemical storage from these data, the rare estimates of soil chemistry are
79 multiplied by the area of land mapped into a specific soil type (Schlesinger 1982, Davidson and
80 LeFebvre 1993, Zhao et al. 2006). Soil chemical analyses can also be grouped by vegetation
81 type (Post et al. 1985) and scaled with a vegetation map, or correlated with independent variables
82 that have well-known regional distributions (Burke et al. 1989).

83 There are several limitations to scaling with soil survey data. In urbanized regions, soil
84 surveys are less useful because urban soils are not surveyed. Agricultural lands are mapped, but
85 often the same soil type will occur on both unmanaged and agricultural land-use types without
86 having separate chemistry values. It is known that for a given soil type, human management can
87 double or halve soil C storage (Kaye et al. 2005, Lewis et al. 2006). Furthermore, because the
88 number of mapped soil types varies with map scale (coarse scale maps usually lump classes from
89 finer scales), several authors (Davidson and LeFebvre 1993; Zhao et al. 2006) have shown that
90 higher resolution maps increase estimates of regional soil C storage. A final shortcoming to
91 simple scaling from soil survey data is that spatial autocorrelation can not be included in the
92 analysis. Several studies have shown that soils display autocorrelation (e.g. Robertson et al.
93 1997), which defines the scale at which values for a soil property are correlated with the values

94 from adjacent points in space. Because soil chemistry is sparsely quantified in soil surveys,
95 spatial autocorrelation can not be calculated.

96 Simulation models can also be used to predict regional distributions of soil carbon and
97 nutrient storage (Burke 2000). They have the advantage of being mechanistically based,
98 increasing the likelihood that predictions will be accurate when the model is extrapolated to new
99 conditions. The problem in applying simulation models to urban ecosystems is that the
100 mechanisms that might be used to simulate urban biogeochemistry have not been established.
101 Kaye et al. (2006) argue that human actions, including landscape design and waste engineering
102 need to be incorporated into urban biogeochemical models. To date, human actions are not
103 dynamic in ecosystem simulation models; actions are defined in prescribed “management” files
104 that are fixed. To simulate human actions, we must first discover the broad patterns that
105 accompany human effects on urban soils and the mechanisms that underlie these patterns.

106 In this paper we present a new approach to modeling the regional distribution of soil
107 organic C (oC), inorganic C (iC), total N, and plant-available P (avP) from plot data. Our
108 approach is based on hierarchical Bayesian regression, which is an empirical (rather than
109 simulation) modeling technique, intended to identify broad patterns in the distribution of soil
110 nutrients across a region of complex land use. Hierarchical Bayes offers several advantages
111 over traditional regression when working on spatially complex ecological problems (Clark
112 2005). First, hierarchical Bayes enables diverse data sources to be used for predicting dependent
113 and independent variables in cases when these data are lacking. This flexibility is especially
114 important in describing urban ecological phenomena that may depend on diverse biophysical and
115 socioeconomic drivers, some of which may only be described at a limited number of sampling
116 points. Second, our model allows multiple regression to be combined with spatial dependence so

117 that variance associated with spatial autocorrelation (which is known to be important for soil
118 properties) can be used in conjunction with variance associated with regression parameters.
119 Finally, hierarchical modeling allows us to couple predictions of soil element pools, allowing a
120 more realistic representation of, for example, the coupled cycles of organic carbon and soil
121 nitrogen.

122 In a previous paper, we outlined the mathematical derivation of a hierarchical Bayesian
123 regression model and its ability to capture variance in soil data from the Phoenix, AZ
124 metropolitan region (Majumdar et al. 2007). Our goals here are to: 1) compare traditional and
125 hierarchical Bayesian approaches to scaling soil nutrients from small plots to the region, 2) use
126 the scaled data to determine the role of humans in changing the distribution of soil carbon and
127 nutrients in the region, and 3) evaluate the significance of the Bayesian model in advancing
128 ecological theory and applications in regions of mixed land use.

129 METHODS

130 *Study site*

131 The research was conducted within and around the Phoenix Metropolitan area of 3.5
132 million people (US Census Bureau, 2000). Natural vegetation is Sonoran desert, but Native
133 American irrigation agriculture was prevalent up to the 1400s and Anglo American agriculture
134 and urbanization have occupied large portions of the region since the 1950s (Fig. 1). Agricultural
135 land is mainly flood irrigated and urban land includes both xeric (desert-like) and mesic
136 landscaping with various modes of irrigation. Annual daily (1948-2003) maximum and minimum
137 temperatures are 30°C and 15°C, respectively and annual average rainfall is 193 mm. The study
138 region was a roughly rectangular area of 7962 km² that includes the city and surrounding
139 agricultural lands and desert (Fig. 1).

140 We use probability-based sampling to acquire a spatially dispersed, unbiased group of
141 sample points from the region (Stevens, 1997; Peterson et al., 1999). A randomized, tessellation-
142 stratified design was achieved by superimposing a 4 km x 4 km grid on the study area, giving
143 462 potential sampling units. We expected high landscape heterogeneity in the urban core (Luck
144 and Wu, 2002), so a random sample point was assigned within every square inside the urban core
145 and in every third square outside that area, giving a total sample size of 206 (Fig. 1). No *a priori*
146 stratification according to land cover, land-use type, or other characteristics was used. A 30m x
147 30m plot was centered on each sample point, regardless of land cover or ownership. Access was
148 granted to all but 8 sites, 6 of these were relocated to the nearest (within 100m) similar accessible
149 site, but for 2 sites access was denied and no suitable surrogate could be found, giving a total of
150 204 sample sites. These 204 sample sites are permanent plots monitored every 5 years by the
151 Central Arizona Phoenix Long-Term Ecological Research Program to assess long term change in
152 a suite of social and biophysical variables. We are reporting on the first soil sample collection in
153 this project, and further details on these plots and their plant and soil properties can be found in
154 Hope et al. (2003, 2005), Zhu et al. (2006), and Oleson et al. (2006).

155 *Soil samples*

156 Soil cores were taken using a hand-impacting corer (2.5 cm diameter to a depth of 30 cm) at four
157 points in each plot (10 m from the randomly selected plot center in all cardinal directions). In
158 cases when these random sampling points fell on an impervious surfaces, the nearest pervious
159 surface was sampled. Core samples were separated into 0-10 cm (top) and 10-30 cm (bottom)
160 depth intervals. Soils from the four cores for each depth were composited and refrigerated. At a
161 small number of survey plots where the entire surface was covered by impervious urban surface,
162 soil samples were collected from the nearest accessible site within 100 meters of the plot

163 boundary. The composite samples were sieved (2 mm) at field moisture, air dried, and
164 homogenized by hand. To determine available P pool sizes, a 10 g subsample of composited soil
165 was extracted with NaHCO_3 , and ortho-phosphate concentrations were determined
166 colorimetrically (Clesceri et al. 1998). A second subsample of composited soil was ground to a
167 fine powder and analyzed for total N and C by dry combustion elemental analysis and for
168 inorganic C by pressure calcimeter (Sherrod et al. 2002).

169 A separate soil core (5 cm diameter by 15 cm deep) was collected at the center of each
170 plot. Particle size distribution in each of these soil cores was determined by the hydrometer
171 method (Gee and Bauder, 1986). Rock-free bulk density was determined by weighing soil that
172 passed through a 2 mm sieve and dividing by volume. The mean density of the < 2 mm fraction
173 ranged from 0.95 g/cm^3 in deserts to 1.14 g/cm^3 in agricultural sites, but did not differ among
174 land-use types (Zhu et al. 2006). Nutrient concentrations from the composite samples (described
175 above) from both depths (0-10 cm; 10-30 cm) were converted to areal density (g/m^2) using the <
176 2 mm soil density from this central core (0-15 cm). Ideally, the bulk density and nutrient
177 concentration data would have been collected from the same depth, but this was not possible
178 because the large diameter core (which is superior for bulk density determination) could not be
179 consistently used at depths below 15 cm. To assess errors arising from this, Zhu et al. (2006)
180 calculated bulk density from a subset of small diameter cores from the 0-10 cm and 10-30 cm
181 depths and found that the ratio (10-30 cm density):(0-10 cm density) was 1.05.

182 *Land use and cover sampling*

183 Many other key biotic, abiotic, and human variables were collected during the field
184 survey. The cover of all ground surface covers (e.g. turf, bare soil and impervious surfaces such
185 as concrete, asphalt, tile, gravel, permanent structures) were mapped using combination of high

186 resolution (1 m) air photos and a field GPS unit (Trimble Pro XL Mapping Grade). Ground
187 cover-types were mapped without overlap, so total aerial coverage was 100%. For the analysis
188 in this paper, we summed the percentage of all impervious surfaces in each plot to calculate our
189 % impervious surface variable. From the pervious surface area, we calculated the percentage of
190 area covered by lawns (ranging from 0 to 100 %) and the percentage of area covered by tree
191 canopies (ranging from 0 to 108 %). Tree canopy area was estimated by measuring the width of
192 the canopy twice (two measurements perpendicular to each other) and calculating the area of a
193 circle with diameter equal to the average of the two field measurements. When canopies
194 extended beyond the plot or originated from stems outside the plot, only the area of the canopy
195 inside the plot was included in the aerial coverage estimate. The irrigated area and type of
196 irrigation on each plot was also recorded. Slope, aspect and elevation were measured. Land use
197 at each of the 204 surveyed sites was classified according to the Maricopa Association of
198 Governments (MAG, 1997) land-use definitions and then modified for compatibility with land-
199 use maps. The main land-use/land-cover categories used in our analysis were: 1) urban
200 residential with xeric vegetation (n = 22), 2) urban residential with mesic vegetation (n = 23), 3)
201 urban residential with a mixture of xeric and mesic vegetation (n = 8), 4) urban non-residential
202 (includes industrial, commercial, transportation, parks, and golf courses; n = 41), 5) water and
203 riparian vegetation (n = 4), 6) desert (n=73), 7) agriculture (n=23), and 8) a mixture of multiple
204 land-use types (n=11).

205 *Scaling approaches*

206 The first challenge in scaling the data described above to the regional scale was the lack
207 of information from soils beneath urban impervious surfaces. We calculated total urban soil
208 pools (pervious plus impervious) using the weighted average of pervious and impervious areas in

209 three ways. First, we assumed that soil pool sizes (g/m^2 of oC, iC, N, and Pav) beneath
210 impervious areas were equal to the pool sizes in the pervious areas we sampled. Second, we
211 assumed that soil pools beneath impervious areas were equal to the desert mean. Third, we
212 assumed that soil pools beneath impervious surfaces were equal to the desert mean for sites with
213 no agricultural history and equal to the agricultural mean for sites that had been cultivated in the
214 past. Using these three data sets, we took two approaches to scaling the 204 data points to the
215 region. The first approach was the “traditional” one of taking the mean value for soil pool sizes
216 (g/m^2) for a given land-use type and multiplying that by the area covered by the land-use type.
217 We compared means ($\alpha = 0.10$) with a one-way ANOVA (land use as the main effect) on the
218 natural logarithm (the data normally distributed following this transformation) of the soils data
219 (iC, oC, N, avP).

220 The area covered by each land-use type was derived from the land-use/land-cover
221 classification of Landsat ETM+ images acquired in the spring of 2000. The classification was
222 created using the National Land Cover Data scheme (<http://www.epa.gov/mrlc/definitions.html>)
223 and the object-oriented hierarchical approach implemented in the eCognition software (Baatz et
224 al. 2003, Moeller 2004). We aggregated several of the land cover categories in this map to 6
225 classes (with aerial coverage in parentheses): 1) urban residential land with xeric landscaping
226 (1607 km^2), 2) urban residential land with mesic landscaping (175 km^2), 3) urban industrial,
227 commercial, and transportation (176 km^2), 4) water and high-density riparian vegetation (9 km^2),
228 5) Sonoran desert (4697 km^2), 6) agricultural land (1130 km^2). This classification scheme
229 matched the Maricopa Association of Governments scheme that we used during our field surveys
230 of the 204 points (described above) except that the remotely sensed land-use map does not
231 include “mixed” land-use categories.

232 The second approach was hierarchical Bayesian scaling that included two steps: (1)
233 develop a regression model that explained variance in soil properties in terms of a limited set of
234 independent variables, and (2) to combine the regression model with spatially explicit data sets
235 for our independent variables to predict soil properties for the entire region. Because
236 hierarchical Bayes is relatively new to ecology and computationally complex, we describe step
237 (1) in detail in Majumdar et al. (2007) and only briefly here. In addition, because of the
238 computational complexity, the Bayesian scaling was only carried out on the top soil layer.

239 *Developing the regression model*

240 All statistical analyses were conducted on the natural logarithm of soil carbon and
241 nutrient concentrations because the raw data were not normally distributed (transformed data
242 were). Model development began by selecting 13 independent variables that included likely
243 geomorphic, ecological, and socio-economic drivers of soil properties: 1) whether the plot was
244 ever used in agriculture or not (a 0 – 1, categorical variable called “ever-in-ag” hereafter), 2)
245 elevation, 3) slope, 4) percent pervious surface area covered by lawn, 5) percent pervious surface
246 area covered by tree canopies, 6) percent of total plot area covered by impervious surfaces, 7)
247 land-use type (a categorical variable with the 8 categories described above), 9) population
248 density, 10) income per capita, 11) irrigation type (a categorical variable with 3 categories: flood,
249 none, other), 12) aspect, and 13) soil texture (percent clay on a soil mass basis). We screened
250 these data using Bayesian information criteria in a simple multiple regression analysis, and seven
251 were significant in explaining the natural logarithm of soil oC, iC, N, and avP content in the
252 surface and deeper soil layers (Table 1).

253 This diverse array of explanatory variables, while realistic, presented a challenge for
254 scaling results from our plots to the region. We did not have spatially explicit regional values for

255 impervious surface (P) and lawn cover (L), so we used Bayesian interpolation (including
 256 stochasticity and spatial autocorrelation), to predict values for these independent variables across
 257 the region. The double natural logarithm was used to transform P and L (e.g. $\ln[\ln(P)]$) to meet
 258 the assumption of normal distributions. From our 204 sample points, we found land-use type
 259 and its interaction with elevation and agricultural history to be strong predictors of impervious
 260 surface and lawn cover (Majumdar et al. 2007).

261 The final model included eight dependent variables (oC, iC, N, and Pav at two soil
 262 depths). To incorporate their association in the model, we used eight levels of hierarchy,
 263 incorporating one extra independent variable at each step. There were also two independent
 264 variables that needed prediction (P and L) and these variables were associated among
 265 themselves, so we modeled their interdependence through another model with two levels of
 266 hierarchy (one for each independent variable being predicted). With ten stochastic processes in
 267 the model (see Table 1 for model variable descriptions) the joint distribution form was

268 $f(Y_1, Y_2, Y_3, Y_4, Y_5, Y_6, Y_7, Y_8, L, P | S, E, \delta, LU, T)$, which we factor as:

269 $f(P | S, E, \delta, LU, T) f(L | P, S, E, \delta, LU, T) f(Y_1 | L, P, S, E, \delta, LU, T) \dots$

270 $\dots f(Y_8 | L, Y_7, Y_6, Y_5, Y_4, Y_3, Y_2, Y_1, L, P, S, E, \delta, LU, T)$ (1)

271 To model the distributions we denote the dependent variables as Y_{ij} , for the i -th variable ($i = 1$ to
 272 8) at the j -th location ($j = 1$ to 204). The spatially random effects, specified by a joint covariance
 273 matrix (Majumdar et al. 2007) are denoted W_{ij} for the i -th dependent variable at the j -th location
 274 or W_{kj} , for the k -th independent variable at the j -th location. Solving for the first distribution, the
 275 % surface area covered by impervious surfaces, we assume that the $\ln(\ln(P_j))$ are conditionally
 276 jointly Gaussian given the S_j, E_j, δ_j, LU_j with the spatially random effect, W_{Pj} , so that P_j are
 277 conditionally independent and identically distributed given S, E, δ , LU, and W_P , giving,

$$278 \quad \ln(\ln(P_j)) | S, E, \delta, W_P \sim N(\beta_{P0} + \beta_{P|S} S_j + \beta_{P|E} E_j + \beta_{P|\delta} \delta_j + \beta_{P|LU} L U_j + W_{P_j}, \sigma_P^2)$$

279 The second distribution, % of pervious area covered by turfgrass lawn, uses similar assumptions.

$$280 \quad \ln(\ln(L_j)) | P, S, E, \delta, LU, W_P \sim N(\beta_{L0} + \beta_{L|P} P_j + \beta_{L|S} S_j + \beta_{L|E} E_j + \beta_{L|\delta} \delta_j + \beta_{L|LU} L U_j + W_{L_j}, \sigma_L^2)$$

281 The last eight distributions, the dependent variables, use similar assumptions and the spatial
282 component is independent Gaussian over i and j , giving,

$$283 \quad Y_{ij} | Y_1, \dots, Y_{i-1}, L, P, S, E, \delta, LU, T, W_1, \dots, W_i \sim N(\beta_{i0} + \beta_{i|1} Y_{1j} + \dots + \beta_{i|i-1} Y_{i-1j} + \beta_{i|P} P_j + \beta_{i|S} S_j + \\ 284 \quad i = 1, 2, 3, 4, 5, 6, 7, 8 \quad \beta_{i|E} E_j + \beta_{i|\delta} \delta_j + \beta_{i|LU} L U_j + \beta_{i|T} T_j + W_{ij}, \sigma_I) \quad (2)$$

285 After fitting the full Bayesian model, the 95% credible interval of the coefficient for “slope”
286 contained zero, so this independent variable was not included in the remaining analyses.

287 Further details regarding the development of the model are in Majumdar et al. (2007). The
288 model was fit to the three soil pool data sets (corresponding to the three assumptions regarding
289 pools beneath impervious surfaces described above) using simulation-based methods, i.e., Gibbs
290 sampling (Gelfand and Smith 1990) and Markov chain Monte-Carlo methods.

291 *Hierarchical Bayesian scaling.*

292 We could have interpolated between our 204 sample points to scale to the region, but the
293 sample plots covered a small fraction of the 6400 km² study region and we felt this sampling
294 intensity was too sparse to justify simple interpolation. Instead, we randomly selected an
295 additional 5000 points from the study area, collected data for 4 independent variables at those
296 points (slope, elevation, ever-in-ag, and current land use), and used the regression model to
297 predict our 2 remaining independent variables (percent area in impervious surfaces and percent
298 of pervious surface covered by lawn) and all dependent variables at each of the 5000 points.
299 Elevation and slope at each of the 5000 points were derived from the 10-meter National
300 Elevation Dataset (NED) assembled by the U.S. Geological Survey

301 (<http://ned.usgs.gov/Ned/about.asp>). The ever-in-ag value (0 or 1) for each site was determined
302 by sampling the time-series of historic land-use maps for 1912, 1934, 1955, 1975, and 1995
303 prepared by the Central Arizona – Phoenix LTER (Knowles-Yanez et al. 1999). Current land
304 use at each site was derived from the same land-cover/land-use map described above (Moeller
305 2004). Once values for the 5000 points were calculated, we used the new points to derive the
306 median and 95% confidence intervals for each major land-use class. By calculating 5000 points
307 instead of 200 we simulate a more complete sampling of our study region and thus, the median
308 values we calculate should better reflect the true median. The medians were transformed from
309 $\ln(\text{g/m}^2)$ to g/m^2 and multiplied by the area occupied by each land-use type.

310 RESULTS

311 *Traditional scaling*

312 Mean surface (0 to 10 cm) oC was lower in desert and xeric lawns (~450 to 500 g/m^2)
313 than in mesic lawns or agroecosystems (750 to 1100 g/m^2 ; Fig. 2). In deeper soils (10 to 30 cm)
314 mean oC was higher in agricultural soils (1020 g/m^2) than in other ecosystems (530 to 730 g/m^2).
315 At both soil depths, desert mean iC (180 g/m^2 at surface and 640 g/m^2 in deeper soil) was lower
316 than all other ecosystems (450 to 620 g/m^2 at surface and 975 to 1040 g/m^2 in deeper soil).
317 Patterns in mean N were similar to oC with mesic lawns and agroecosystems having 75 to 125
318 g/m^2 more N in the top 30 cm of soil than xeric lawns or desert. Mean avP to 30 cm was also
319 greater in mesic lawns and agroecosystems (3.8 to 4.7 g/m^2) than in other ecosystems (1.8 to 2.4
320 g/m^2). When these mean values were multiplied by the aerial extent of the land-use types (Fig.
321 1a), deserts contained the largest pools of all elements in the region, followed by xeric lawns and
322 agriculture, and then mesic lawns and non-residential urban areas (Fig. 3). The values were
323 relatively insensitive to our assumptions regarding soils beneath impervious surfaces in the urban

324 environment (Fig. 3). If we assume that prior to human development, the entire region had mean
325 element storage similar to the mean of our desert samples ($n = 73$), then the top 30 cm of soil in
326 all the human dominated ecosystems (all urban + agricultural) have accumulated 1140 Gg (350
327 g/m^2) of oC, 1280 Gg (390 g/m^2) of iC, 130 Gg (39 g/m^2) of N, and 3.6 Gg (1.1 g/m^2) of avP in
328 the top 30 cm of soil (Table 3).

329 *Bayesian scaling*

330 Ecologists generally use the mean as the measure of central tendency (thus, data in the
331 prior section are discussed in terms of means) because ANOVA analyses compare means, or
332 more broadly because ecologists are most comfortable with Gaussian distributions, where the
333 mean is an accurate description of central tendency. Our Bayesian analysis compared medians
334 so we facilitate comparisons by plotting median values from the data beside the median values
335 from the 5000 points generated by the model. Modeled estimates of median oC in the top 10 cm
336 of soil (Fig. 4) followed roughly the same pattern as data means (Fig. 2) for mesic lawns, urban
337 non-residential land, and deserts. However, for xeric lawns, modeled estimates of median oC
338 (824 g/m^2) were about twice as great as the data median or mean. In contrast, for agricultural
339 ecosystems, modeled oC (450 g/m^2) was 30 to 40 % of the data mean or median. These
340 differences in estimated central tendency lead to proportional differences in region-wide
341 estimates of soil oC storage (Fig. 5 vs. Fig. 3). Estimates of region-wide oC storage in
342 agricultural soils were lower from the Bayesian model (540 Gg) than from data means (868 Gg).
343 In contrast, model estimates of oC storage in xeric lawns (1633 Gg) were about twice as great as
344 the value (860 Gg) from a traditional scaling approach. The model suggests that xeric lawns that
345 cover about 20 % of the land area account for as much oC storage as deserts that cover 59% of
346 the land area. Our assumptions regarding storage beneath urban impervious surfaces had a large

347 impact on the estimate of regional oC storage in xeric residential areas (Fig. 5), but this
348 assumption can not account for differences between Bayesian and traditional scaling approaches.
349 Summing over all ecosystems that we analyzed, the Bayesian model (4460 Gg) was similar to
350 the traditional approach (4210 Gg) in estimating soil oC in the top 10cm (Table 3).

351 Modeled median iC values for all urban land-use types (230 to 296 g/m²) were lower than
352 data medians and means (350 to 650 g/m²; Figs. 2 and 4). In deserts and agricultural ecosystems
353 modeled median iC was higher than the data median and lower than the data mean. When scaled
354 to the region, differences between the Bayesian and traditional approaches were most apparent in
355 xeric lawns and deserts (Fig. 5 vs Fig. 3). Bayesian estimates of iC in xeric lawns (362 Gg) and
356 desert soils (563 Gg) are 60 and 67 % of the values generated by the traditional scaling approach.
357 Summing over all the land-use types that we analyzed, Bayesian scaling estimates 1490 Gg of
358 region-wide iC storage in surface soils while the traditional scaling estimates 2160 Gg (Table 3).

359 The data and model medians were similar for N and avP in all ecosystems (Fig. 4).
360 Likewise, for N and avP, the Bayesian and traditional scaling approaches produced similar
361 estimates of regional soil storage in the top 10 cm (Table 3).

362 Geostatistical modeling of the 5000 points used in our Bayesian scaling analysis allowed
363 us to produce spatially continuous maps of soil carbon and nutrient storage across the region
364 (Fig. 1). We applied the ordinary cokriging interpolator and used land-use codes as the second
365 variable in semivariogram modeling. The maps show that oC, N, and avP share spatial
366 patterning throughout the city; all are highest in urban and agricultural areas and lowest in the
367 desert. In contrast iC, which is predicted with elevation, is highest in the southwestern portion of
368 the study area and declines abruptly as elevation increases near isolated mountains or gradually
369 as elevation increases toward the northeastern part of the study area.

370 DISCUSSION

371 *Traditional versus Bayesian approaches*

372 One of our main objectives was to compare traditional and hierarchical Bayesian
373 approaches to scaling. The Bayesian model is computationally complex; to justify the effort, the
374 model must represent a significant improvement over the simple spreadsheet calculations
375 required for traditional scaling. The two approaches generated similar results for soil N and avP
376 for both the distribution among land-use types (Fig. 2 vs Fig 4) and the total regional stocks
377 (Table 3). For soil C pools the results were more complex. The Bayesian approach predicts
378 greater oC storage in xeric lawns and lower oC storage in agricultural soils than the traditional
379 approach leading to comparable estimates of region-wide oC storage between the two methods.
380 The model consistently predicted lower iC storage than data means, leading to a much lower
381 estimate of region-wide iC storage (Table 3).

382 Two factors likely account for the differences between the Bayesian and traditional
383 approaches in their predictions of oC and iC. First, it is well known that soil properties display
384 spatial autocorrelation, that is, that the value for soil properties at one location is correlated with
385 values from nearby locations (Robertson et al. 1997). While the variance explained by spatial
386 autocorrelation can not be attributed to measured independent variables, it can be taken into
387 account when predicting soil properties at new points in the landscape. Hierarchical Bayes
388 allowed us to compute the spatial structure of the data to increase the portion of data variance
389 explained by the model and inform interpolation for region-wide scaling. In our data from 34 to
390 55 % of the unexplained variance in our regression model was due to spatial autocorrelation
391 (Table 2). In the traditional scaling approach this variance is not taken into account.

392 The second factor that accounts for differences between methods was the use of multiple
393 regression in the Bayesian approach. The traditional scaling approach assumed that 1) most of
394 the soil variance in the region is attributable to one factor - contemporary land use, and 2) that
395 the mean of our soil samples was representative of the mean value for a given land-use type in
396 our region. Our Bayesian regression analysis shows that the first assumption was violated (Table
397 2) and allowed us to include a diverse array of biophysical and socioeconomic independent
398 variables predict soil properties. We also modeled the dependent variables simultaneously, so
399 that our predictions of oC concentrations were improved by their correlation with N. With
400 strong predictive power (Table 2), we were able to simulate soil properties at 5000 points and
401 use these data to estimate the central tendency for each land-use type. This new estimate of
402 central tendency should be closer to the “true” value because it accounts for the variance
403 attributable to several factors (independent variables, spatial autocorrelation, and correlation with
404 other dependent variables) that are not taken into account when the simple mean from our 200
405 data points is multiplied by land-use area.

406 Given these qualitative differences between the scaling methods it is not surprising that
407 our estimates of regional nutrient storage differed between the Bayesian and traditional
408 approaches. We believe the Bayesian estimates should be closer to the “true” values for the
409 reasons described above. Yet, the limitations of time and computational effort are substantial.
410 The bottom layer of soil contains a significant amount of C and we chose not to apply Bayesian
411 scaling to these data due to the computational burden.

412 *Distribution of soil carbon and nutrients in a human-dominated region.*

413 Despite differences among the scaling methods, there are some generalities that can be
414 discerned regarding the regional distribution of soil C, N, and P. First, oC, N, and avP appear to

415 be highly correlated (Table 2; Fig. 1). Urban mesic lawns contain more oC, N, and avP per
416 square meter than other ecosystems and all human dominated (agricultural plus urban)
417 ecosystems contain more of oC, N, and avP than deserts. Deserts still dominate the aerial
418 coverage of the region (59% using our land-use map; Fig. 1), but account for only 38 - 40 % of
419 regional oC and iC stocks and 51-52 % of regional N and Pav stocks in surface soils (0 to 10 cm)
420 using the Bayesian scaling approach (Fig. 5). Results from the traditional scaling approach are
421 similar (Fig. 3), with desert carbon and nutrient stocks in the 0 to 30 cm depth accounting for 48
422 to 53 % of the regional total. While the relative importance of the desert versus human
423 dominated land-use types is totally dependent on our choice of regional boundaries, it is still
424 significant that in our relatively large (6400 km²) study region, the “slow” variables of soil C and
425 N stocks have been altered. Because soil oC, N, and avP are tightly linked in soils through
426 biological processing, their correlation at the regional scale with human-dominated landscapes
427 suggest that humans are altering regional soil properties by altering biological nutrient cycling.

428 While the distribution of oC, N, and avP seem related to human manipulation of
429 biogeochemistry, the pattern for iC is not so clear. Both scaling approaches suggest that iC is
430 higher in all human-dominated ecosystems than in deserts. One interpretation for this pattern is
431 that salt inputs from irrigation water lead to the accumulation of iC in soil (Schlesinger 1985,
432 1999). Irrigation water in this region can be saturated with CaCO₃ (L. Baker, unpublished data),
433 which precipitates out of solution as water is removed in the root zone, concentrating salts in the
434 high CO₂ environment of the soil. However, our Bayesian regression analysis did not find
435 irrigation presence or type to be an important predictor of iC, in fact, no independent variables
436 corresponding to human management were good predictors of iC, only elevation and latitude
437 were significant (Table 2). At this point, we can not determine whether urban and agricultural

438 development happened to occur on soils with high iC, or whether management practices lead to
439 iC accumulation. However, in desert soils of this region, high iC accumulation is associated with
440 older surfaces on higher elevation terraces. Thus, if natural pedogenic processes were driving
441 regional iC distribution we would have expected a positive correlation between iC and elevation,
442 which is the opposite of our data pattern.

443 Our estimates of regional soil C and N storage can be compared to previous studies of N
444 and C fluxes in the same study region. Baker et al. (2001) constructed a budget of N fluxes for
445 the same region and found 17 to 21 Gg of N per year that could not be accounted for. They
446 assumed that this N was accumulating somewhere in the region because inputs and outputs were
447 well constrained. Zhu et al. (2006) suggested that 46 Gg of soil inorganic N had accumulated in
448 the region's soils (mainly in urban and agricultural soils). Here we calculate (Table 3) that 130
449 Gg N accumulated in the top 30 cm of soil of human-dominated ecosystems. Together, these
450 results suggest that: 1) soil N accumulation accounts for < 8 years ($130 \text{ Gg} / 17 \text{ Gg yr}^{-1} = 7.6 \text{ yr}$)
451 of the N that was unaccounted for in the budget of Baker et al. (2001), and 2) that a large fraction
452 of the accumulating soil N is inorganic ($46 \text{ Gg inorganic N} / 130 \text{ Gg total N} = 0.35$). Additional
453 N is likely stored in the vadose zone and in underlying groundwater (Baker et al. 2001). Urban
454 ecosystems have very large N inputs compared to unmanaged ecosystems (Kaye et al. 2006).
455 Our results suggest that urban soils are an important sink for urban N at regional and decadal
456 scales. Retention of N in soils mitigates the effects of imported urban N on water and air quality
457 and future research on the longevity and stability of urban soil N will be needed to understand
458 variability in urban N pollution.

459 Koerner and Klopatek (2002) evaluated the distribution of CO₂ sources in our study
460 region. Vehicles accounted for 80 % of regional CO₂ emissions, but soil respiration (15%) was

461 the second largest source of CO₂ emissions. They found that deserts (~180 gCm⁻²yr⁻¹) and xeric
462 residential sites (~400 gCm⁻²yr⁻¹) had low soil respiration rates compared to agricultural land
463 (2000 to 3000 gCm⁻²yr⁻¹) and urban mesic lawns (~2500 gCm⁻²yr⁻¹). Coupling these soil
464 respiration estimates with our soil C data enables us to make preliminary calculations regarding
465 land-cover effects on the mean residence time of C in soils (Schlesinger 1977, McCulley et al.
466 2004). If between 33 and 67 % of soil respiration is from heterotrophic microbial respiration,
467 then the mean residence time of soil C in deserts (8.5 to 17 y) and xeric residential soils (3.4 to
468 7.2 y) is much longer than in agricultural (1 to 3 y) and urban mesic (1 to 2 y) soils. These
469 preliminary calculations underestimate C residence times because they only included soil C to 30
470 cm. Adding deeper soil C (Schlesinger 1982) to the calculation could double or triple our
471 estimates of mean residence time, but probably would not change relative differences between
472 land-use types because deeper soil C varies less with land management than surface C (Fig. 2;
473 Kaye et al. 2005). Raich and Schlesinger (1992) used a similar approach to calculate the mean
474 residence time of soil C for whole biomes and the shortest mean residence times occurred in
475 tropical grasslands (~ 10 years). Thus, even after tripling the mean residence time to account for
476 deep soil C, agricultural and urban mesic soils in our study region have very short C residence
477 times compared to other ecosystems. We are currently examining multi-pool estimates of soil C
478 residence times to increase our understanding of soil-atmosphere gas exchange in Phoenix
479 residential soils.

480 *Conclusion: using Bayesian models to advance ecology in mixed-use regions.*

481 We used a single statistical model to predict soil properties simultaneously across a wide
482 variety of land-use types in central Arizona, USA. We achieved large scale predictability by
483 modeling traditional ecological parameters and socioeconomic variables that reflect human

484 actions. One of the emerging tenets of urban ecological theory is that human actions must be
485 included in models of urban ecosystem functioning (Kaye et al. 2006) and our statistical model
486 provides support for this idea; human choices regarding lawn design, impervious surface cover,
487 and tree cover were all significant predictors of soil element distributions. While values of
488 regional soil element stocks are important for understanding our regional ecosystem (see below),
489 an equally important result, in terms of advancing the ecology of mixed-use landscapes, are maps
490 (Fig. 1b-e) that portray soil properties of the region as subtle and dramatic gradients spanning all
491 ecosystem types. These images (and the model that produced them) better represent the
492 connectedness of landscape components than traditional models that use discrete land-use or soil
493 type boundaries to depict landscape soil patterns.

494 Hierarchical Bayes enabled this seamless cross-system analysis, and we suggest that
495 Bayesian modeling could be a key tool for an ecology that spans ecosystems. Our model
496 includes four major advances over traditional ecological approaches. First, it enabled us to use
497 diverse types of data to predict soil properties. This flexibility is important when both
498 biophysical and socioeconomic factors may be driving environmental change. Second, we
499 include spatial autocorrelation in our predictions of regional soil pools. Spatial autocorrelation
500 explains a large fraction of variance in soil pools at small scales (Robertson et al. 1997), but has
501 not previously been invoked to map regional patterns of soil carbon and nutrient distributions.
502 Third, hierarchical Bayes allowed us to predict values for independent variables at points where
503 data are lacking, and used variance in the existing data to generate confidence intervals for our
504 estimates of regional storage. Traditional scaling approaches are limited to interpolating only at
505 points where values for independent variables have been quantified. Finally, we modeled the
506 joint distributions of oC, iC, N, and avP, which is consistent with the idea of coupling of

507 biogeochemical processes in ecosystems. The model predicts spatial coupling of biologically
508 mediated pools (oC, N, and avP) across this diverse landscape, despite the myriad human
509 impacts on regional soils.

510 Our results have several implications for urban land managers. In general, our data show
511 that soils are an important component of city-scale C, N, and P budgets and that some urban soils
512 store more C, N, and P than adjacent deserts. Thus, as cities strive to mitigate air and water
513 pollution, soil element accumulation may play a role. An important caveat is that our study did
514 not fully account for the costs and longevity of soil element storage. For example, in Phoenix,
515 high soil C, N, and Pav storage occurs in mesic residential areas with high turfgrass cover. These
516 landscapes are associated with high irrigation and fertilizer inputs, a short mean residence time
517 for soil C, and high gaseous N losses (Zhu et al. 2004). Thus, the overall environmental benefits
518 of soil element storage may not be significant relative to environmental costs that we did not
519 measure.

520 We also found that variability in urban soil element storage is correlated with cultural
521 variables that reflect land development and management choices. In Phoenix, choices regarding
522 the location of development affect urban element storage because urban plots on former
523 agricultural fields had higher C and N storage than plots on former deserts (Tables 1 and 2;
524 Lewis et al. 2006). Choices about the amount of impervious cover, turfgrass lawn cover, and
525 tree cover were also correlated with soil N, P, and C storage. These are urban characteristics that
526 are often managed by individual home owners, but they were important predictors of city-wide
527 element storage.

528 ACKNOWLEDGEMENTS

529 This material is based upon work supported by the National Science Foundation under
530 Grant No. DEB-0423704 [Central Arizona - Phoenix Long-Term Ecological Research (CAP
531 LTER)], the NSF Ecosystem Studies Program (DEB-0514382; N.B.G., and DEB-0514379;
532 J.P.K.), and the NSF Biocomplexity in the Environment Program (EAR-0322065; L.A.B and
533 J.P.K.). Any opinions, findings and conclusions or recommendation expressed in this material
534 are those of the author(s) and do not necessarily reflect the views of the National Science
535 Foundation (NSF).

536 LITERATURE CITED

- 537 Aber J., W. McDowell, K. Nadelhoffer, A. Magill, G. Berntson, M. Kamakea, S. McNulty, W.
538 Currie, L. Rustad, and I. Fernandez. 1998. Nitrogen saturation in temperate ecosystems.
539 *Bioscience* 48:921-934.
- 540 Anderson, J., E. Hardy, J. Roach, and R.E. Witmer. 1976. A Land Use and Land Cover
541 Classification System for Use with Remote Sensor Data. Geological Survey Professional
542 Paper 964.
- 543 Baatz, M., U. Benz, S. Dehghani, M. Heyen, A. Höltje, P. Hofmann, I. Lingenfelder, M. Mimler,
544 M. Sohlbach, M. Weber, and G. Willhauck. 2003. eCognition software user guide.
545 Definiens Imaging GmbH, München, Germany.
- 546 Baker, L.A., D. Hope, Y. Xu, Y., L. Lauver, and J. Edmonds. 2001. Nitrogen balance for the
547 Central Arizona-Phoenix Ecosystem. *Ecosystems* 4, 582-602.
- 548 Brown, J.H., J.F. Gillooly, A.P. Allen, V.M. Savage, and G.B. West. 2004. Toward a metabolic
549 theory of ecology. *Ecology* **85**: 1771–1789.

- 550 Burke I.C., C.M. Yonker, W.J. Parton, C.V. Cole, K. Flach, D.S. Schimel. 1989. Texture,
551 climate, and cultivation effects on soil organic matter content in U.S. grassland soils. Soil
552 Science Society of America Journal 53:800-805.
- 553 Burke, I.C. 2000. Landscape and regional biogeochemistry: Approaches. *In* Sala, O, R.
554 Jackson, H. Mooney, and R. Howarth, eds. *Methods in Ecosystem Science*. New York:
555 Springer, New York. Pp. 277-287.
- 556 Clark, J. 2005. Why environmental scientists are becoming Bayesians. *Ecology Letters* 8: 2-14.
- 557 Clesceri, L.S., A.E. Greenburg, and A.D. Eaton, editors. 1998. *Standard Methods for the*
558 *examination of water and wastewater* 20th ed. Prepared and Published jointly by APHA,
559 AWWA and WEF. United Book Press, Inc. Baltimore, MD.
- 560 Davidson, E.A. and P.A. LeFebvre. 1993. Estimating regional carbon stocks and spatially
561 covarying edaphic factors using soil maps at three scales. *Biogeochemistry* 22:107-131.
- 562 Ellison, K. 2006. Cities take on climate change. *Frontiers in Ecology and the Environment* 4:
563 336.
- 564 Gee, G.W., and J.W. Bauder. 1986. Particle size analysis. Pages 383-411 in A. Klute, editor,
565 *Methods of soil analysis, part 1. Physical and Mineralogical Methods*. 2nd ed. Agron.
566 Monogr. 9 ASA and SSSA, Madison, WI..
- 567 Gelfand, A. E., and A.F.M. 1990. Sampling based approaches to calculating marginal densities.
568 *J. Am. Stat. Assoc.* 85, 398-409.
- 569 Hope, D. *et al.* 2003. Socioeconomics drive urban plant diversity. *Proc. Natl. Acad. Sci. U.S.A.*
570 100, 8788-8792.

- 571 Hope, D., W. Zhu, C. Gries, J. Oleson, J.P. Kaye, N.B. Grimm, and L. Baker. 2005. Spatial
572 variation in inorganic soil nitrogen across an arid urban ecosystem. *Urban Ecosystems*
573 8:251-273.
- 574 Jenerette, D., J. Wu, N. Grimm and D. Hope. 2006. Points, patches and regions: Scaling soil
575 biogeochemical patterns in an urbanized arid ecosystem. *Global Change Biology*
576 12:1523-544.
- 577 Kaye, J.P., R. McCulley, and I.C. Burke. 2005. Carbon fluxes, nitrogen cycling and soil
578 microorganisms in adjacent urban, native and agricultural ecosystems. *Global Change*
579 *Biology* 11:575-587.
- 580 Kaye, J.P., P. Groffman, N.B. Grimm, L. Baker, and R. Pouyat. 2006. A distinct urban
581 biogeochemistry? *Trends in Ecology and Evolution* 21:192-199.
- 582 Knowles-Yáñez, K., C. Moritz, J. Fry, M. Bucchini, C.L. Redman, and P. McCartney. 1999.
583 Historic land use team: Phase I report on generalized landuse. Central Arizona-Phoenix
584 LTER: Phoenix, Arizona, USA.
- 585 Koerner, B., and J. Klopatek. 2002. Anthropogenic and natural CO₂ sources in an arid urban
586 environment. *Environmental Pollution* 116: S45-S51.
- 587 Levin, S.A. 1992. The problem of pattern and scale in ecology. *Ecology* 73: 1943-1967
- 588 Lewis, D., J.P. Kaye, C. Gries, A. Kinzig, and C. Redman. 2006. Agrarian legacy in soils of
589 urbanizing aridlands. *Global Change Biology* 12: 703-709.
- 590 Luck, M.A. and J. Wu.. 2002. A gradient analysis of the landscape pattern of urbanization in the
591 Phoenix metropolitan area of USA. *Landscape Ecology* 17, 327-339.

- 592 Majumdar, A., J.P. Kaye, C. Gries, D. Hope, R. Burdick, and N. Grimm. 2007. Hierarchical
593 spatial modeling of multivariate soil nutrient concentrations in heterogenous land-use
594 patches of the Phoenix metropolitan area. *Communications in Statistics* (in press).
- 595 Maricopa Association of Governments. 1997. *Urban Atlas, Phoenix Metropolitan Area*.
596 Maricopa Association of Governments, Phoenix, AZ.
- 597 McCulley, R.L., S.R. Archer, T.W. Boutton, F. Hons, and D.A. Zuberer. 2004. Soil respiration
598 and nutrient cycling of wooded communities developing in grassland. *Ecology* 85: 2804-
599 2817
- 600 Moeller, M. 2004. Multi-Temporal Remote-Sensing Data Acquisition for CAP LTER Land
601 Cover/Land Use Monitoring and Modeling: SAVI (Modified Soil Adjusted vegetation
602 index) Image of 2003 ASTER image.
603 <http://caplter.asu.edu/home/products/datasetByIpa.jsp>
- 604 Okin, G. S., N. Mahowald, O.A. Chadwick, O.A., and P. Artaxo. 2004. Impact of desert dust on
605 the biogeochemistry of phosphorus in terrestrial ecosystems. *Glob. Biogeochem. Cycles*
606 **18**: Art. No. GB2005. [doi: 10.1029/2003GB002145].
- 607 Oleson, J., D. Hope, C. Gries, and J.P. Kaye. 2006. A Bayesian approach to estimating regression
608 coefficients for soil properties in land-use patches with varying degrees of spatial
609 variation. *Environmetrics* 17: 517-525.
- 610 Pacala, S.W., G.C. Hurtt, D. Baker, P. Peylin, R.A. Houghton, R.A. Birdsey, L. Heath, E.T.
611 Sundquist, R.F. Stallard, P. Ciais, P. Moorcroft, J.P. Caspersen, E. Shelvliakova, B.
612 Moore, G. Kohlmaier, E. Holland, M. Gloor, M.E. Harmon, S.-M. Fan, J.L. Sarmiento,
613 C.L. Goodale, D. Schimel, and C.B. Field. 2001. Consistent Land- and Atmosphere-
614 Based U.S. Carbon Sink Estimates. *Science* 292:2316-2320.

- 615 Peterjohn, W. T., and D. L. Correll. 1984. Nutrient dynamics in an agricultural watershed:
616 observations on the role of a riparian forest. *Ecology* **65**: 1466–1475.
- 617 Peterson, S.A., N.S. Urquhart, and E.B. Welch. 1999. Sample representativeness: a must for
618 reliable regional lake condition estimates. *Environ. Sci. Technol.* 33, 1559-1565.
- 619 Post, W.M., J. Pastor, P.J. Zinke, and A.G. Stangenberger. 1985. Global patterns of soil nitrogen
620 storage. *Nature* 317: 613–616
- 621 Ptacnik, R., G.D. Jenerette, A.M. Verschoor, A.F. Huberty, A.G. Solimini, and J.D. Brookes.
622 2005. Applications of ecological stoichiometry for sustainable acquisition of ecosystem
623 services. *Oikos* 109: 52_ 62.
- 624 Raich, J.W. and W.H Schlesinger. 1992. The global carbon dioxide flux in soil respiration and its
625 relationship to vegetation and climate. *Tellus* 44B: 81–99
- 626 Reppert, B. 2006. Global warming: Congress still stalled, states and cities act. *Bioscience* 56:
627 800.
- 628 Robertson, G.P., K. Klingensmith, M. Klug, E. Paul, J. Crum. 1997. Soil resources, microbial
629 activity and primary production across and agricultural ecosystem. *Ecological*
630 *Applications* 7: 158-170.
- 631 Schlesinger, W.H. 1977. Carbon balance in terrestrial detritus. *Ann. Rev. Ecol. Systematics* 8:
632 51–81.
- 633 Schlesinger, W.H. 1982. Carbon storage in the caliche of arid soils: a case study from Arizona.
634 *Soil Science* 133:247-255.
- 635 Schlesinger, W.H. 1985. The formation of caliche in soils of the Mojave Desert, California.
636 *Geochimica et Cosmochimica Acta*, 49, 57-66.

- 637 Schlesinger, W.H. 1999. Carbon and agriculture: carbon sequestration in soils. *Science*, 284,
638 2095.
- 639 Sherrod, L., G. Dunn. and G. Peterson. 2002. Inorganic carbon analysis by modified pressure
640 calcimeter method. *Soil Science Society of America* 66: 299-305.
- 641 Stevens, D.L. Jr. 1997. Variable density grid-based sampling designs for continuous spatial
642 populations. *Environmetrics* 8, 167-195.
- 643 U.S. Census Bureau. 2000. Phoenix-Mesa metropolitan statistical area population
644 demographics., <http://www.census.gov>.
- 645 Zhao, Y., X. Shi, D. Weindorf, D. Yu, W. Sun, and W. Hongjie. 2006. Map Scale Effects on
646 Soil Organic Carbon Stock Estimation in North China. *Soil Sci. Soc. Am. J.* 70:1377–
647 1386
- 648 Zhu, W.X., N.D. Dillard, and N.B. Grimm. 2004. Urban Nitrogen Biogeochemistry: status and
649 processes in green retention basins. *Biogeochemistry* 71: 177-196
- 650 Zhu, W-X., D. Hope, C. Gries,, and N.B. Grimm. 2006. Soil Characteristics and the
651 Accumulation of Inorganic Nitrogen in an Arid Urban Ecosystem. *Ecosystems* 9: 711-
652 724.

653

Table 1. Notations of variables used in the model

Y_1	\ln (g total nitrogen/m ²) in the 0 to 10 cm depth
Y_2	\ln (g organic carbon/m ²) in the 0 to 10 cm depth
Y_3	\ln (g inorganic carbon/m ²) in the 0 to 10 cm depth
Y_4	\ln (g available phosphorus/m ²) in the 0 to 10 cm depth
Y_5	\ln (g total nitrogen/m ²) in the 10 to 30 cm depth
Y_6	\ln (g organic carbon/m ²) in the 10 to 30 cm depth
Y_7	\ln (g inorganic carbon/m ²) in the 10 to 30 cm depth
Y_8	\ln (g available phosphorus/m ²) in the 10 to 30 cm depth
S	slope (degrees)
E	elevation (meters)
δ	= 0 if never in agriculture; = 1 if ever used for agriculture
P	% surface area covered by impervious surfaces
L	% of pervious area covered by turfgrass lawn
LU	Land-use category
T	% of pervious area covered by tree canopies
W	spatially random effects
j	unique spatial location
β	Regression coefficients
σ^2	Random error variance

654

655
656

Table 2. Results of the Bayesian regression analysis of factors correlating with soil pools.

Soil pools	Significant regression coefficients	Correlation between modeled and measured values	Fraction of unexplained variance attributed to spatial autocorrelation
<i>Surface layer (0 to 10 cm)</i>			
oC	Surface layer N % surface area covered by impervious surfaces	0.94	0.48
iC	Elevation	0.87	0.42
N	Ever in agriculture % of pervious area covered by turfgrass lawn	0.94	0.35
avP	Surface layer N	0.89	0.55
<i>Deeper layer (10 to 30 cm)</i>			
oC	Deeper layer N Surface layer oC	0.88	0.41
iC	Surface layer iC Latitude Elevation	0.95	0.45
N	Surface layer iC Surface layer N % of pervious area covered by turfgrass lawn % of pervious are covered by trees	0.91	0.46
avP	Surface layer oC Deeper layer oC Surface layer avP Latitude	0.85	0.34

657

658

Table 3. Regional soil carbon and nutrient stocks and the potential amount (a subset of the total stock) attributable to net accumulation in urban and agricultural ecosystems in Gg.

Soil Depth	Scaling Approach	oC	iC	N	avP
----- <i>Total region stocks</i> -----					
0 to 10 cm	Bayesian	4460	1490	477	8
0 to 10 cm	Traditional	4210	2160	540	8
10 to 30 cm	Traditional	5140	5790	730	11
0 to 30 cm	Traditional	9360	7950	1270	18
<i>Potential accumulation in urban and agricultural ecosystems</i>					
0 to 10 cm	Bayesian	1350	470	55	0.9
0 to 10 cm	Traditional	540	680	50	1.4
10 to 30 cm	Traditional	600	600	80	2.1
0 to 30 cm	Traditional	1140	1280	130	3.6

659

660 Figure 1. Maps of landuse (panel a), and soil carbon or nutrient pools (panels b-e) in the study
661 region. In all maps red lines are major roads. Soil maps were generated by interpolating
662 between 5000 points where carbon and nutrient content were estimated using the Bayesian
663 regression model.

664

665 Figure 2. Mean soil carbon and nutrient pools in common land-use types of the study region
666 from 204 measured points. Bars are means (n = 22 to 73) and standard error of the 0 to 30 cm
667 depth. Different lower case letters within a bar denote statistical differences ($p < 0.10$) among
668 land-use types for the 0 to 10 or 10 to 30 cm depths, while lowercase letters above bars denote
669 statistical differences for the 0 to 30 cm.

670

671 Figure 3. Soil carbon and nutrient storage in common land-use types of the study region
672 calculated using the means from 204 measured points (Fig. 2) and the aerial extent of land-use
673 (i.e. traditional scaling approach). There are no error estimates for these values because we have
674 no error estimates for the aerial extent of land-use (Fig. 1a). For the urban ecosystems, bars
675 reflect the assumption that storage beneath impervious surfaces depends on agricultural history
676 (see methods), the symbol x is the value assuming impervious surface pools are equal to desert
677 pools, and the symbol ♦ is the value assuming that impervious pools are equal to pervious pools
678 at the same plot.

679

680 Figure 4. Median soil carbon and nutrient pools (0 to 10 cm depth) in common land-use types of
681 the study region calculated from data (from 204 measured points) or the hierarchical Bayesian

682 model (from 5000 points predicted by the regression model). Bars are medians ($n = 22$ to 73)
683 and errors show the 2.5 and 97.5 percentiles.

684

685 Figure 5. Soil carbon and nutrient storage (0 to 10 cm depth) in common land-use types of the
686 study region derived from 5000 estimates predicted with the Bayesian regression model (i.e. the
687 Bayesian scaling approach). There are no error estimates for these values because we have no
688 error estimates for land area coverage (Fig. 1a). For the urban ecosystems, bars reflect the
689 assumption that storage beneath impervious surfaces depends on agricultural history (see
690 methods), the symbol \times is the value assuming impervious surface pools are equal to desert pools,
691 and the symbol \blacklozenge is the value assuming that impervious pools are equal to pervious pools at the
692 same plot.

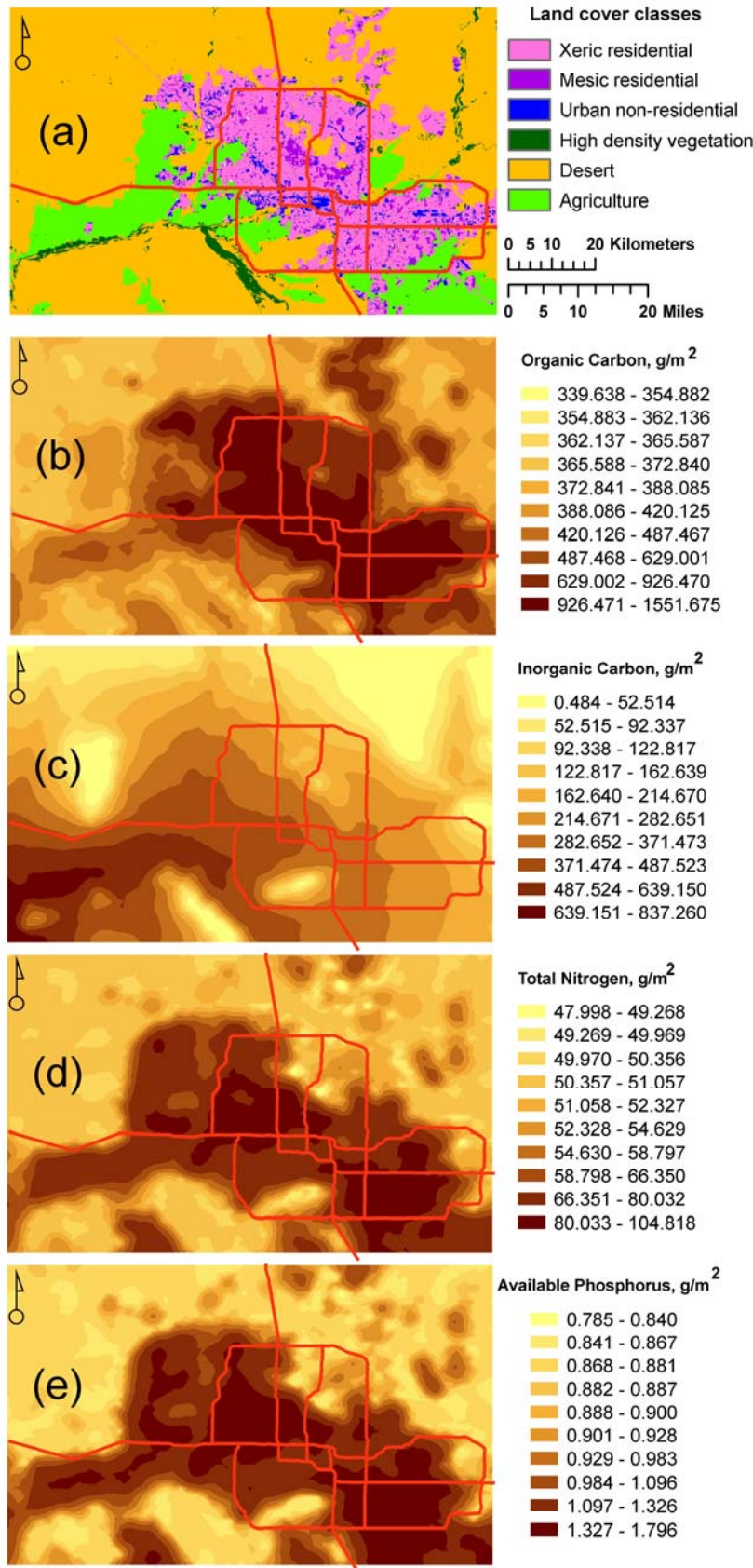
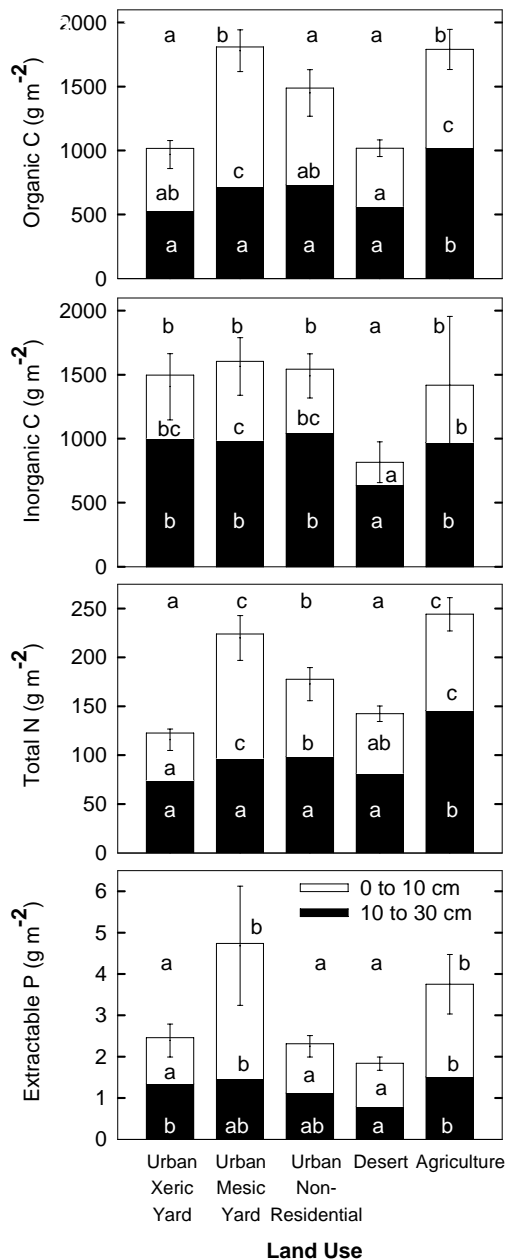
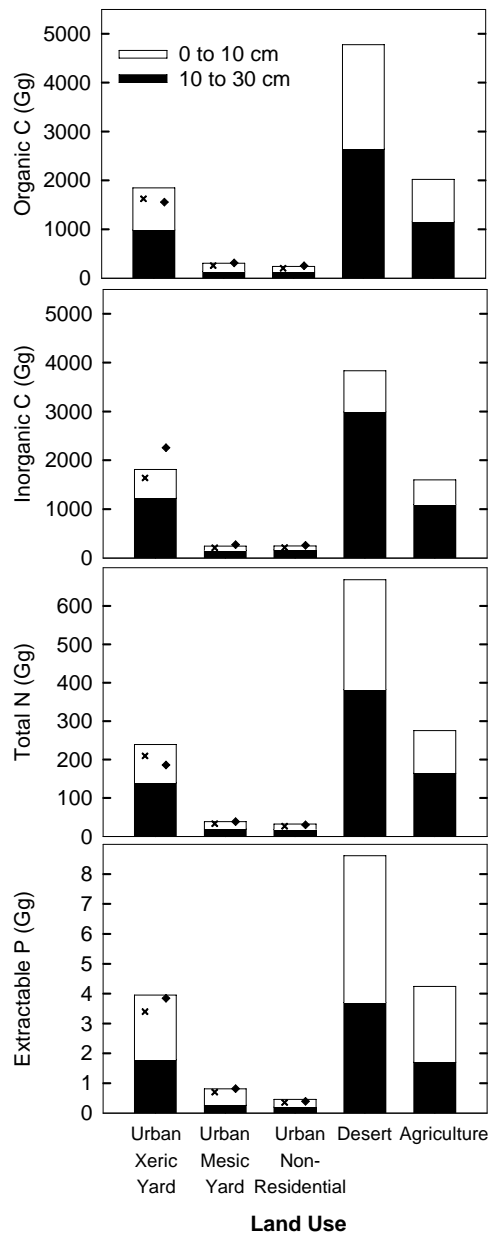


Figure 1. Maps of landuse (panel a), and soil carbon or nutrient pools (panels b-e) in the study region. In all maps red lines are major roads. Soil maps were generated by interpolating between 5000 points where carbon and nutrient content were estimated using the Bayesian regression model.



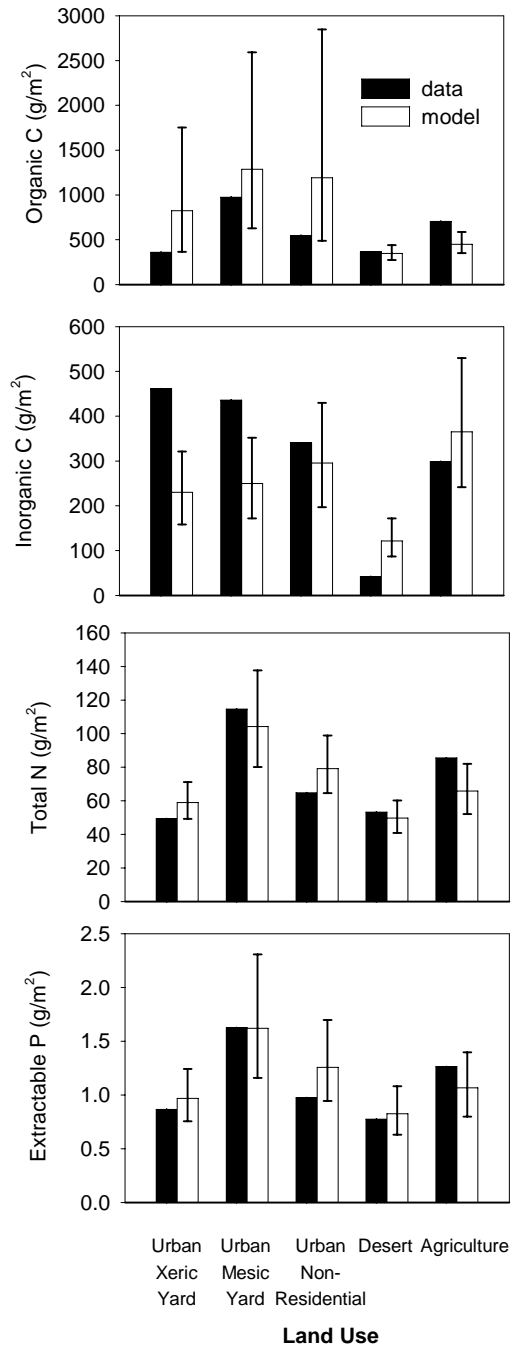
705
706
707
708
709
710

Figure 2. Mean soil carbon and nutrient pools in common land-use types of the study region from 204 measured points. Bars are means (n = 22 to 73) and standard error of the 0 to 30 cm depth. Different lower case letters within a bar denote statistical differences (p < 0.10) among land-use types for the 0 to 10 or 10 to 30 cm depths, while lowercase letters above bars denote statistical differences for the 0 to 30 cm.



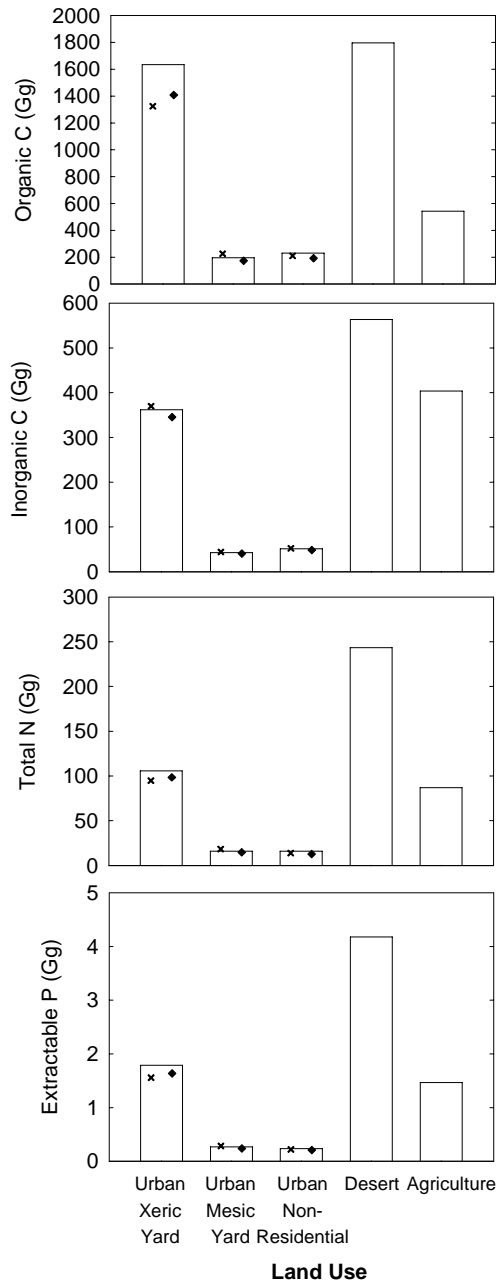
711
712
713
714
715
716
717
718
719
720

Figure 3. Soil carbon and nutrient storage in common land-use types of the study region calculated using the means from 204 measured points (Fig. 2) and the aerial extent of land-use (i.e. traditional scaling approach). There are no error estimates for these values because we have no error estimates for the aerial extent of land-use (Fig. 1a). For the urban ecosystems, bars reflect the assumption that storage beneath impervious surfaces depends on agricultural history (see methods), the symbol x is the value assuming impervious surface pools are equal to desert pools, and the symbol ♦ is the value assuming that impervious pools are equal to pervious pools at the same plot.



721
722
723
724
725
726

Figure 4. Median soil carbon and nutrient pools (0 to 10 cm depth) in common land-use types of the study region calculated from data (from 204 measured points) or the hierarchical Bayesian model (from 5000 points predicted by the regression model). Bars are medians (n = 22 to 73) and errors show the 2.5 and 97.5 percentiles.



727
728

729 Figure 5. Soil carbon and nutrient storage (0 to 10 cm depth) in common land-use types of the
 730 study region derived from 5000 estimates predicted with the Bayesian regression model (i.e. the
 731 Bayesian scaling approach). There are no error estimates for these values because we have no
 732 error estimates for land area coverage (Fig. 1a). For the urban ecosystems, bars reflect the
 733 assumption that storage beneath impervious surfaces depends on agricultural history (see
 734 methods), the symbol x is the value assuming impervious surface pools are equal to desert pools,
 735 and the symbol ♦ is the value assuming that impervious pools are equal to pervious pools at the
 736 same plot.